# UNIVERSITY OF BIRMINGHAM

## University of Birmingham Research at Birmingham

### Initial stiffness and plastic resistance of bolted stainless steel T-stubs in tension

Yuan, Huanxin; Gao, Jundong; Theofanous, Marios; Yang, L; Schafer, Benjamin

DOI:

10.1016/j.jcsr.2020.106239

License

Creative Commons: Attribution-NonCommercial-NoDerivs (CC BY-NC-ND)

Document Version
Peer reviewed version

Citation for published version (Harvard):

Yuan, H, Gao, J, Theofanous, M, Yang, L & Schafer, B 2020, 'Initial stiffness and plastic resistance of bolted stainless steel T-stubs in tension', *Journal of Constructional Steel Research*, vol. 173, 106239. https://doi.org/10.1016/j.jcsr.2020.106239

Link to publication on Research at Birmingham portal

General rights

Unless a licence is specified above, all rights (including copyright and moral rights) in this document are retained by the authors and/or the copyright holders. The express permission of the copyright holder must be obtained for any use of this material other than for purposes permitted by law.

- •Users may freely distribute the URL that is used to identify this publication.
- •Users may download and/or print one copy of the publication from the University of Birmingham research portal for the purpose of private study or non-commercial research.
- •User may use extracts from the document in line with the concept of 'fair dealing' under the Copyright, Designs and Patents Act 1988 (?)
- •Users may not further distribute the material nor use it for the purposes of commercial gain.

Where a licence is displayed above, please note the terms and conditions of the licence govern your use of this document.

When citing, please reference the published version.

Take down policy

While the University of Birmingham exercises care and attention in making items available there are rare occasions when an item has been uploaded in error or has been deemed to be commercially or otherwise sensitive.

If you believe that this is the case for this document, please contact UBIRA@lists.bham.ac.uk providing details and we will remove access to the work immediately and investigate.

Download date: 13. Mar. 2024

### Initial stiffness and plastic resistance of bolted stainless steel T-stubs in

2 tension

3 H. X. Yuan<sup>a,\*</sup>, J. D. Gao<sup>a</sup>, M. Theofanous<sup>b</sup>, L. Yang<sup>c</sup>, B.W. Schafer<sup>d</sup>

<sup>a</sup> Hubei Provincial Key Laboratory of Safety for Geotechnical and Structural Engineering, School of Civil Engineering, Wuhan University, Wuhan 430072, PR China

<sup>b</sup> Department of Civil Engineering, University of Birmingham, Birmingham B15 2TT, United Kingdom

<sup>c</sup> The College of Architecture and Civil Engineering, Beijing University of Technology, Beijing 100124, PR China

<sup>d</sup> Department of Civil Engineering, Johns Hopkins University, Baltimore, MD 21218, United States

Corresponding author:

Dr Huanxin Yuan, School of Civil Engineering, Wuhan University, Wuhan 430072, China. Email: <a href="mailto:yuanhx@whu.edu.cn">yuanhx@whu.edu.cn</a>

Abstract: Building upon a previous investigation, this study reports a total of 13 experimental tests on austenitic and duplex stainless steel T-stubs subject to monotonic loading. The structural behaviour of the tested T-stub specimens, including load versus displacement (F- $\Delta$ ) curves and corresponding failure modes, was obtained and is reported herein. The experimental tests were replicated by finite element (FE) analysis, and upon validation of numerical models, a comprehensive parametric study including 168 FE models was conducted to investigate the effects of key parameters such as material grade, bolt preloading, bolt diameter and flange thickness on the structural response. Based on both experimental and numerical results, the suitability of the design provisions for the determination of the plastic resistance specified in EN 1993-1-8, proposed extensions thereof by Demonceau et al. to cover T-stubs with four bolts per row for stainless steel T-stubs as well as the design method codified in Chinese code JGJ 82 were assessed. Novel design methods for the determination of the initial stiffness and the plastic resistance of stainless steel T-stubs, accounting explicitly for the observed structural response and the pronounced material strain hardening were developed. The proposed design methods lead to improved and more consistent capacity predictions and their adoption in design standards is recommended herein.

Keywords: Stainless steel; T-stub; Bolted connection; Initial stiffness; Plastic resistance; Design method

#### 1 Introduction

Basic components of bolted beam-to-column joints, such as column flange in bending and end plate in bending are traditionally modelled using equivalent T-stubs in tension, within the framework of the component method. The load-carrying capacity of structural steel T-stub connections were thoroughly studied by many scholars. Douty and McGuire [1] conducted 27 T-stub tests by using a universal testing machine and derived a predictive model for prying forces, whilst Struik and de Back [2] developed a simplified model accounting for the prying effect of T-stubs, which served as the basis of the EN 1993-1-8 design provisions [3]. Later, Zoetemeijer [4] reported testing and analytical studies on carbon steel T-stub flanges in bolted beam-to-column connections, and Jaspart [5] derived design methods for predicting the stiffness and resistance of T-stubs that were later incorporated into the Eurocode 3 [3]. More tests on steel T-stubs have emerged over the past two decades, with the research work conducted by Swanson et al. [6,7], Piluso et al. [8-10] and Girão Coelho et al. [11,12] enabling a better understanding of the structural behaviour of steel T-stubs. More recently, Wang et al. [13] presented numerical studies on strength and initial stiffness of steel T-stubs with blind bolts and Liu et al. [14,15] tested 10 steel T-stub connections to examine the influence of the employed geometric configurations, and provided semi-empirical calculation formulae for T-stubs. Furthermore, T-stubs made of high strength steel were investigated by Zhao et al. [16] and Chen et al. [17], and the applicability of the design provisions in EN 1993-1-8 were verified based on the obtained experimental and numerical results. Ten additional T-stubs in

grade Q690 high strength steel connections were tested by Guo et al. [18] and Liang et al. [19], and it was revealed that the design method for T-stubs presented in EN 1993-1-8 [3] could be extended to cover the Q690 steel grade, yet an alternative simplified analytical approach was proposed to acquire more accurate predictions of the initial stiffness of high strength steel T-stubs. In addition, Demonceau et al. [20] presented design formulae of steel T-stubs with four bolts per horizontal row based on the EN 1993-1-8 provisions, and Latour et al. [21] modified the formulae for all possible collapse mechanisms of T-stubs with four bolts per row based on experimental and numerical investigations.

Special attention has been paid to the structural behaviour of T-stubs made of nonlinear metallic materials. The tensile behaviour of aluminium alloy T-stub connections was investigated and reported in [22-25], wherein modifications to the design method provided in EN 1999-1-1 [26] were proposed. Meanwhile, a relatively small number of studies on the behaviour of stainless steel T-stub connections has been conducted to date. Bouchaïr et al. [27] examined numerically the ultimate resistance and development of prying forces of stainless steel T-stubs and provided a comparison between stainless steel and carbon steel T-stubs. A total of 28 austenitic stainless steel T-stubs with a single bolt row were tested under monotonic loading by Yang [28] and Lei [29], followed by parallel numerical modelling of the structural behaviour. Tests on 27 stainless steel T-stubs of both austenitic and duplex grades were reported in [30,31], based on which, the existing design methods initially proposed for carbon steel T-stubs, which are also applicable to stainless steel [32] T-stubs were evaluated and were found to provide overly conservative resistance predictions. Moreover, the structural performance of stainless steel beam-to-column joints was studied for both conventional bolted beam-to-column joints [33-36] and blind bolted beam-to-column joints [37,38], and it was observed that the plastic moment resistance of the tested joints was consistently and significantly underestimated by EN 1993-1-8 [3].

Experimental tests on 13 stainless steel T-stub connections in tension were conducted and are reported herein, which together with 27 tests on stainless steel bolted T-stub connections previously reported [30] and 28 test results reported in [28,29] constitute an experimental pool of 68 tests on austenitic grade EN 1.4301 and duplex grade EN 1.4462 stainless steel T-stubs. All test results are used herein to assess existing design rules for stainless steel joints specified in EN 1993-1-8 [3], JGJ 82 [39], as well as the method proposed by Demonceau et al. [20] for T-stubs with 4 bolts per row. Advanced FE models are initially developed using ABAQUS and validated against available test data. Based on the validated FE models, parametric studies are conducted and 168 FE models are generated to investigate the influence of key parameters on the overall structural response, strength and failure modes. Finally, design recommendations for the initial stiffness and the plastic resistance of stainless steel T-stubs in tension are made. The proposed design equations lead to more accurate strength and stiffness predictions and are well-suited for incorporation in future revisions of existing design guidance.

#### 2 Experimental study

#### 2.1 Test specimens

A total of 13 stainless steel T-stub connections were tested. These are classified in 3 geometric configurations, namely T-S, T-D and T-F as shown in Fig. 1. Both the austenitic grade EN 1.4301 (ASTM 304) and the duplex grade EN 1.4462 (ASTM 2205) were employed, whilst the chosen bolt classes included A4-70 and A4-80 stainless steel bolts. Controlled tightening by means of a calibrated wrench was used to apply bolt preloading to a specified level, as preloading was one of the key parameters, the influence of which on the structural response is investigated herein. The measured geometric dimensions of all tested specimens are listed in Table 1, where  $d_b$  is bolt nominal diameter,  $h_f$  is the fillet weld size and  $F_{pre}$  is the applied bolt preloading force measured with calibrated load cells.

#### 2.2 Material properties

The material properties of the stainless steel plates and bolts of the T-stub specimens were experimentally determined from standard tensile coupon tests. To this end, rectangular and round coupons were machined from hot-

rolled plates and bolts respectively and were tested to failure. The full stress-strain curves have been reported in [30], whilst the average values of the material properties including the Young's modulus  $E_0$ , the 0.01%, 0.2%, 1.0% and 3.0% proof stresses, the tensile strength  $\sigma_u$ , the strain hardening exponent n, and the plastic strain at fracture  $\varepsilon_f$  for each tested coupon are summarised in Table 2.

#### 2.3 Test results

A detailed description of the employed experimental setup and instrumentation is given in [30]. All tests were conducted to failure which in all cases was triggered by bolt fracture. The recorded axial load (F) versus displacement ( $\Delta$ ) curves from the 13 test specimens reported herein are shown in Fig. 2. The experimentally obtained plastic resistance ( $F_{Rd}$ ) defined as the load at the intersection between the initial stiffness line and the tangent line of the hardening part, together with the ultimate resistance ( $F_u$ ) at the peak point of test curve, are summarised in Table 3, where the corresponding deformations  $\Delta_{Rd}$  and  $\Delta_u$  at which  $F_{Rd}$  and  $F_u$  occur are also reported. The points ( $\Phi_{Rd}$ ) and ( $\Phi_u$ ) are denoted in Fig.2 with a white and a black circle respectively. It can be seen that the ultimate resistance  $F_u$  can be more than four times the plastic resistance  $F_{Rd}$  for some specimens, whilst the deformation  $\Phi_u$  at  $\Phi_u$  is can be more than ten times that at  $\Phi_u$  as can also be seen in Fig. 2, demonstrating the significant deformation capacity of the tested specimens.

The deformed shapes of the tested T-stub specimens are illustrated in Fig. 3. It is noted that the deformed shape of specimen F13s is not provided due to inability to disassemble the specimen after testing. As expected, all specimens failed ultimately by bolt fracture, but the deformation that the T-stubs sustained until bolt fracture occurred depended strongly on the flexural strength of the T-stubs relative to the tensile strength of the bolts. It can be observed that specimens employing thinner flanges, stronger bolts and larger bolt spacing m display significantly larger plastic deformations compared to specimens with thicker plates, smaller bolts and smaller bolt spacing m. This observation is directly reflected in the F- $\Delta$  curves shown in Fig. 2. Curves (Fig. 2) displaying a significantly higher ultimate resistance  $F_{\rm u}$  compared to their plastic resistance  $F_{\rm Rd}$  are associated with failure modes (Fig. 3) exhibiting large plastic deformations. For example, specimens S10s and S11s can be seen in Fig. 2 to exhibit a significant difference between  $F_{\rm Rd}$  and  $F_{\rm u}$  (i.e. significant steepness of the force-displacement curve beyond the knee region) and significant plastic deformations of the flanges in Fig. 3. On the contrary, specimens S12s and S14s display a less steep force-displacement curve beyond the knee region of their F- $\Delta$  curves reported in Fig. 2, and this corresponds to failure modes involving almost straight flanges as can be observed in Fig. 3.

The correlation between high plastic deformations and significant overstrength beyond the plastic resistance of the T-stubs can be attributed to the combined effects of material strain hardening at the locations of the yield lines and the development of membrane action in the flanges at high deformations. This is clearly seen in the load-displacement curves of specimens S10s, S11s, D9s, D10s, F11s and F13s, which display an increase in stiffness at high deformations, which can only be attributed to the change of response of the flanges to accommodate the applied load from predominantly flexural to predominantly tensile. The effect of membrane actions on the T-stub response is more pronounced for T-stubs employing thin flanges, large spacing *m* and strong bolts that can allow significant deformation of the T-stub flanges and anchor the developed tension field prior to fracture. Hence, T-stubs failing in mode 1 are expected to possess significantly higher overstrength compared to their counterparts failing in mode 2 or mode 3.

#### 2.4 Comparison with resistance predictions from the existing design methods

The existing design methods for T-stubs made of carbon steels include the design formulae provided in EN 1993-1-8 [3] and Chinese code JGJ 82 [39], which are based on the prying model developed by Struik and de Back [2]. These design standards are applicable to stainless steel T-stubs and are evaluated herein by comparing their predictions against an experimental pool consisting of 68 test results. For the comparison, the measured geometric and material properties are utilised and all safety factors are set to unity. The related calculation formulae for determining the plastic resistance in EN 1993-1-8 are given by Eqs. (1)-(3) corresponding to the three typical failure modes of T-stubs with two bolts per row (T-S and T-D configurations).

Mode 1 T-S, T-D and T-F 
$$F_{1,Rd} = \frac{(8n - 2e_{w})M_{pl,1,Rd}}{2mn - e_{w}(m+n)}$$
 (1)

Mode 2 T-S and T-D 
$$F_{2, Rd} = \frac{2M_{pl, 2, Rd} + n\sum F_{t, Rd}}{m+n}$$
 (2)

Mode 3 T-S, T-D and T-F 
$$F_{3,Rd} = \sum F_{t,Rd}$$
 (3)

- where  $e_w$  is equal to  $d_w/4$  ( $d_w$  is the diameter of the washer), m and n are indicated in Fig. 1,  $M_{pl,1,Rd}$  and  $M_{pl,2,Rd}$  are the plastic moment resistances of the T-stub flange based on the material yield strength  $f_y$  and can be calculated using Eq.
- 133 (4), and  $F_{t,Rd}$  is the tension resistance of a bolt given by Eq. (5).

$$M_{\text{pl,i,Rd}} = \frac{t_f^2 f_y}{4} \sum l_{\text{eff,}i} \quad i=1 \text{ or } 2$$
 (4)

$$F_{t,Rd} = 0.9 f_{ub} A_s \tag{5}$$

- where  $t_f$  and  $f_y$  are the thickness and yield strength of T-stub flange,  $\sum l_{eff,i}$  (i=1 or 2) is the calculated effective length for the corresponding failure mode,  $A_s$  and  $f_{ub}$  are the tensile stress area and ultimate tensile strength for bolts, respectively.
- Moreover, Demonceau et al. [20] proposed a design method for T-stub connections with four bolts per horizontal row (T-F) in the framework of the design provisions in EN 1993-1-8, which employs Eq. (6) for mode 2 but still adopts Eqs. (1) and (3) for failure modes 1 and 3, respectively.

Mode 2 T-F
$$F_{2, Rd} = \frac{2M_{f, 2, Rd} + \frac{\sum F_{t, Rd}}{2} \left( \frac{n_1^2 + 2n_2^2 + 2n_1 n_2}{n_1 + n_2} \right)}{m + n_1 + n_2}$$
(6)

in which the geometric symbols m,  $n_1$  and  $n_2$  are indicated in Fig. 1.

145

146

147

148

149

150

151

152

153

154

155156

157

158 159

The design equations in the Chinese code JGJ 82 [39] are given by Eqs. (7) and (8) in a rewritten form.

Modes 1 and 2 T-S and T-D 
$$N_{\rm t, 1-2} = \sum \frac{b_{\rm c} f_{\rm y} (1 + \delta \alpha') t_{\rm f}^2}{4e_2}$$
 (7)

Mode 3 T-S and T-D 
$$N_{t,3} = \sum f_{ub} A_s$$
 (8)

- where  $b_c$  is the calculated width for each bolt row,  $e_2$  is the distance from bolt centreline to the web,  $\delta$  and  $\alpha'$  are two calculation coefficients related to the geometric dimensions of T-stubs, and the term  $1 + \delta \alpha'$  is used to account for the prying effect.
  - The design method codified in the AISC manual [40] is not included in the following discussion due to the fact that it aims to estimate the ultimate resistance rather than the plastic resistance of T-stubs by introducing the ultimate tensile stress of flange instead of the yield strength. This paper focuses on the plastic resistance of the T-stubs, which is suitable for conventional design. The ultimate response of T-stubs, which may be relied upon in accidental load cases and is strongly dependent on the development of membrane action will be discussed in future publications.
  - Table 3 reports the experimentally obtained and predicted plastic resistances of the T-stubs considered, as well as their ratios. A ratio less than 1.0 indicates unsafe design predictions. The specimens employing four bolts per row are utilised only for the assessment of EN 1993-1-8 [3] as adapted in [20]; they are not considered when assessing the JGJ 82 equations, as this configuration is not covered therein. It is evident that both design methods in EN 1993-1-8 and JGJ 82 provide overly conservative resistances, and the average ratios are equal to 1.40 and 1.75 for the 13 tests reported in this paper with corresponding standard deviations of 0.14 and 0.33, respectively. A similar level of accuracy is demonstrated when the 27 tests reported in [30] are considered. The EN 1993-1-8 predictions are slightly improved when assessed based on the 28 T-stub tests reported by Yang [28] and Lei [29], whilst the Chinese code JGJ 82 [39] predictions appear to be even more conservative. The average ratios from all 68 available tests are 1.36 and 1.96 for the design methods in EN 1993-1-8 and JGJ 82 with corresponding standard deviations of 0.13 and 0.36, respectively.

The conservatism exhibited by both design codes considered relates to neglecting the effect of strain hardening and adopting the nominal yield strength of the flange as the limiting stress attainable by the T-stubs. For materials lacking a yield plateau and exhibiting pronounced strain hardening such as stainless steels the adoption of  $f_y$  as a limiting stress value leads to overly conservative strength predictions. This statement is supported by the observation that the plastic resistance of the austenitic stainless steel specimens is more severely underpredicted compared to the plastic resistance of their duplex stainless steel counterparts, which can be attributed to the more pronounced strain hardening inherent in austenitic stainless steels. It is thus concluded that the development of more accurate and efficient design methods accounting for the effect of strain hardening is required. To this end, a comprehensive parametric study on stainless steel T-stubs is conducted hereafter.

#### 3 Numerical modelling

#### 3.1 Development of FE models

Numerical models simulating the tested stainless steel T-stub connections were developed by means of the general purpose FE software package ABAQUS. Three individual parts representing the stainless steel T-stub, the stainless steel bolt and steel block were created. All components of the bolt assembly, namely shank, head and nut were simulated as smooth cylinders, with the shank diameter selected such as to achieve a cross-sectional area equal to the stress area of the threaded bolt. The fillet welds were assumed to be part of the T-stub. Due to the symmetry of the T-stubs in terms of geometry, boundary conditions and applied loads, only one half of each tested specimen was modelled, as shown in Fig. 4, thereby significantly reducing the computational cost. All parts of the models were meshed with the eight-node linear first-order brick element C3D8I. This element is enhanced by incompatible modes to improve the bending behaviour and has 8 integration points and 13 internal degrees of freedom [41], thereby enabling more accurate stress and strain results. Following a mesh convergence study to obtain a suitable element size for a satisfactory balance between accuracy and computational efficiency, the general element sizes for the T-stub and bolts were set at 3 mm and 1.5 mm, respectively. A finer mesh was employed in the vicinity of expected regions of stress concentration such as the bolt hole to accurately capture the expected steep stress gradients. The typically generated number of elements of the T-S, T-D and T-F models are 15000, 28000 and 25000, respectively.

The nonlinear material behaviour of stainless steel T-stubs and bolts was modelled assuming the standard von Mises yield criterion with isotropic hardening. The engineering stress-strain curves obtained from the tensile coupon tests (reported in Ref. [30]) were converted to true stress and logarithmic plastic strain and input in ABAQUS to quantify hardening. While the behaviour of the steel block was assumed elastic and was modelled assuming a Young's modulus of 206 GPa and a Poisson's ratio of 0.3.

The boundary conditions were defined to reflect the support conditions employed in the experimental tests. All degrees of freedom of the bottom surface of the steel block were restrained, and symmetry boundary conditions were applied to the mid-thickness plane of the web. A vertical displacement was prescribed at the top of the web to simulate displacement control loading. The experimentally measured bolt preloading force was introduced by using the BOLT LOAD command, and it was found that the presence of a small bolt preload for snug tightened conditions improved the convergence behaviour, as it eliminated initial slip of the bolt holes.

The adopted contact interactions are shown in Fig. 4, wherein the surface-to-surface formulation with finite sliding was defined between adjacent surfaces. The normal behaviour was simulated assuming hard contact, and the tangential response of contact surface was modelled by the classical isotropic Coulomb friction model with penalty method [42]. The friction coefficient was taken as 0.2 for the two contact pairs including the steel block and the flange, the steel block and the bolt nut, while the friction coefficient of the other contact pair – the flange and the bolt nut was set equal to 0.15 [43]. It has been noted that the effect of the friction coefficients turns out to be insignificant for stainless steel bolted T-stubs in tension based on a sensitivity analysis as the deformations of the model do not induce significant tangential contact. Meanwhile, the tangential behaviour of contact between the bolt shank and the hole wall was

assumed to be frictionless [19].

#### 205 3.2 Validation

The developed FE models were utilised to replicate numerically a total of 40 tests reported herein and in Ref. [30]. A general static analysis allowing for geometric and material nonlinearities was conducted. The comparison between the numerical predictions and the test results in terms of the obtained F- $\Delta$  curves and the failure modes of typical specimens are presented in Fig. 5. It can be observed that the numerically predicted load-deformation curves are in close agreement with the test curves. Moreover, the deformed shapes of the T-stubs obtained from numerical modelling agree well with the experimental results, as indicated in Fig. 5.

The numerically predicted plastic and ultimate resistances together with corresponding deformation values at which these occur for all 40 T-stubs are compared with the test results, as shown in Table 4. The average values of  $F_{\rm Rd,Exp}/F_{\rm Rd,FE}$  and  $F_{\rm u,Exp}/F_{\rm u,FE}$  ratios are calculated to be 1.03 and 1.02 with small standard deviations of 0.06 and 0.03, respectively, and the mean ratios of  $\Delta_{\rm Rd,Exp}/\Delta_{\rm Rd,\,FE}$  and  $\Delta_{\rm u,Exp}/\Delta_{\rm u,\,FE}$  are equal to 0.96 and 0.99 with slightly higher standard deviations. Besides, the initial stiffness of T-stubs obtained from numerical modelling are also compared with the experimental values, as shown in Table 6. Based on the close agreement between FE modelling and testing, the developed FE models are deemed able to accurately capture the behaviour of stainless steel bolted T-stubs in tension, and are therefore utilised in subsequent parametric studies.

#### 3.3 Numerical study of failure modes

It is known that the three typical failure modes of carbon steel bolted T-stubs specified in EN 1993-1-8 are the complete yielding of the flange (Mode 1), the bolt failure with yielding of the flange (Mode 2) and the bolt failure only (Mode 3), based upon which the plastic tension resistances of T-stubs are derived using the material yield strength of the flange and the tension resistance of bolt. However, the failure mechanisms of stainless steel T-stubs may differ from those made of ordinary carbon steels in view of the significant material non-linearity of stainless steel plates and bolts, which are numerically studied herein.

Both the flange bending moment close to flange-to-web intersection and the bolt tension force corresponding to the plastic resistance were obtained for all the 40 T-stubs, and are tabulated in Table 5. It can be seen that the numerically obtained flange bending moments  $(M_{\rm pl-FE})$  are considerably higher than the plastic moment resistances  $(W_{\rm pl}f_{0.2})$ calculated by using the nominal material yield strength  $f_{0.2}$ , indicating the significant effect of the strain hardening capacity of stainless steel. Meanwhile, the stress distributions through flange thickness corresponding to the plastic resistance, located close to the flange-to-web intersection, were attained and are plotted in Fig. 6 for all three types of T-stub connections, where the stress values are normalised by the 3.0% proof strength ( $\sigma_{3.0} = f_{3.0}$ ) of the flange material. It is shown that the stress amplitudes of both tensile and compressive regions for all the three types of T-stubs are close to the  $\sigma_{3.0}$ , which is much higher than the nominal yield strength  $\sigma_{0.2}$  (see Table 2). By comparing the numerically obtained flange bending moments ( $M_{\rm pl-FE}$ , corresponding to the plastic resistance) with the plastic moments calculated by using material strength  $f_{3.0}$ , the mean value of the  $M_{pl-FE}/(W_{pl}f_{3.0})$  ratio is equal to 1.00 with a corresponding standard deviation of 0.05, as shown in Table 5. Moreover, the numerical bolt tension forces  $F_{t-\text{FE}}$  are also compared to the tension resistance  $A_{s}f_{ub}$ . By referring to the definition of the three typical failure modes, it can be concluded that the failure mode 2 implies that both flange moment and bolt tension force ratios are close to 1.00, and the failure mode 1 corresponds to the flange moment ratio roughly equal to 1.00 but with a much smaller bolt tension force ratio, while the failure mode 3 suggests the bolt tension force ratio reaches 1.00 with a generally lower flange moment ratio. The failure modes of all 40 T-stub connections were hence determined as either failure mode 1 or 2 and are given in Table 5. It is noted that the bolt tension force ratios for both the inner and outer bolts are included for the T-stubs with four bolts per row (T-F), and it is revealed that failure of the outer bolt cannot be expected in the failure mode 1 and most cases with the failure mode 2.

According to the design formulae provided in EN 1993-1-8 [3], the theoretical relationship between the plastic resistance of T-stubs ( $F_{\rm Rd}$ ) and flange thickness squared ( $t_{\rm f}^2$ ) can be represented in Fig. 7. Specifically, the plastic resistance  $F_{\rm Rd}$  is proportional to the square of the thickness of the T-stub  $t_{\rm f}^2$  for failure mode 1, whist the resistance for mode 3 is independent of the flange thickness, since it essentially involves only failure of the bolt. For T-stubs displaying mode 2 mechanism, a weaker correlation is found between  $F_{\rm Rd}$  and  $t_{\rm f}^2$  compared with the mode 1, as shown in Fig. 7, as mode 2 involves failure of both the bolt and the flange of the T-stub.

Four different values of the bolt diameter  $d_b - 12$  mm, 16 mm, 20 mm and 24 mm were chosen to examine the relationship between  $F_{Rd}$  and  $t_f^2$  for T-stubs made of austenitic grade EN 1.4301 and duplex grade EN 1.4462, and the obtained numerical results are plotted in Fig. 8, which are found to be consistent with the theoretical one given in Fig. 7. It is evident that stainless steel T-stubs display similar failure mechanisms falling into the three typical modes in EN 1993-1-8, as shown in Fig. 9 for a typical T-S model, though the stresses at plastic flange yielding reach up to the 3.0% proof strength which is much higher than the nominal material yield strength. Introducing larger bolt diameter can considerably raise the tension resistance of T-stubs, especially for those displaying failure modes 2 and 3. As expected, increasing flange thickness results in the change of failure mode, as illustrated in Fig. 9. Besides, the T-stubs with flanges made of the duplex grade EN 1.4462 exhibit higher tension resistances compared to the austenitic counterparts having the same flange thickness due to the considerably higher material strength.

#### 3.4 Numerical study of initial stiffness

From the experimental tests it was concluded that the introduction of bolt preloading generated a considerable increase in the initial stiffness of T-stubs, while it had little effect on the resistance and deformation capacity. The developed FE models were re-run without bolt preloading forces to quantify the influence of preloading on the initial stiffness. The effect of preloading on initial stiffness is illustrated in Fig. 10, where the ratio of the initial stiffness of every T-stub with preloaded bolts is normalised by the initial stiffness of the same T-stub but without bolt preloading. It is shown that the initial stiffness of preloaded T-stubs is increased by 53% on average due to the introduction of bolt preloading forces up to 60% of bolt ultimate resistance, compared to their non-preloaded counterparts, indicating the significant effect of bolt preloading on the initial stiffness regardless of the type of T-stub and the bolt grade involved. It is noted that the beneficial effect of preloading on initial stiffness is more pronounced with decreasing flange stiffness and becomes less significant when the flexural stiffness of the T-stub flange increases. Similar conclusions were previously reached by other scholars for carbon steel T-stubs [44,45].

Moreover, the sensitivity of the initial stiffness to the ratio  $\rho$  of the bolt preloading force  $(F_{\text{pre}})$  over the bolt ultimate resistance  $(f_{\text{ub}}A_{\text{s}})$  was explored by considering seven different values ranging from 0 to 0.6, in which  $\rho$ =0 corresponding to the snug tightened condition. The comparison of the initial parts of the obtained numerical load versus displacement curves for typical T-stub models is plotted in Fig. 11, which refers to specimen S8 in [30]. The three typical failure modes were achieved by setting three different flange thickness values (11.85 mm, 16 mm and 30 mm). It can be clearly seen that higher values of  $\rho$  result in increased initial stiffness regardless of the exhibited failure mode, but the influence becomes less pronounced with the ratio  $\rho$  greater than 0.4. Additionally, it is also shown that the bolt preloading has little effect on the tension resistance of T-stubs.

#### 3.5 Parametric studies

The previously validated FE models were further used to investigate the effect of key parameters, such as material grade, bolt diameter and flange thickness on the structural behaviour of the T-stubs. The range of the flange thickness considered varied from 4 mm to 40 mm, and the bolt diameter varied from 12 mm to 24 mm. A total of 168 numerical models of T-stub connections employing the T-S, T-D and T-F configurations were generated to cover both austenitic and duplex grades and are utilised in the following section to verify a proposed design method.

#### 289 4 Design recommendations

#### 290 4.1 Determination of initial stiffness

Several calculation methods for computing the initial stiffness ( $K_0$ ) of T-stub connections exist. In EN 1993-1-8 [3], the initial stiffness of a T-stub connection can be obtained from its basic components using Eq. (9):

$$K_0 = \frac{1}{\frac{1}{K_t} + \frac{1}{K_b}} \tag{9}$$

in which  $K_t$  and  $K_t$  are the initial stiffnesses of the T-stub and the bolts respectively, and can be computed for each single bolt row by Eqs. (10) and (11), which are applicable to both preloaded and non-preloaded connections.

$$K_{t} = \frac{0.9E_{0,t}l_{\text{eff}}t_{f}^{3}}{m^{3}} \tag{10}$$

$$K_{b} = \begin{cases} \frac{1.6E_{0,b}A_{s}}{L_{b}} & \text{for failure modes 1 and 2} \\ \frac{2.0E_{0,b}A_{s}}{L_{b}} & \text{for failure mode 3} \end{cases}$$
 (11)

where  $E_{0,t}$  and  $E_{0,b}$  are the Young's moduli of the T-stub plates and bolts, respectively;  $l_{eff}$  is the effective length for each bolt row;  $A_s$  and  $L_b$  represent the tensile stress area and elongation length of the bolt, respectively. Besides, the coefficient 1.6 in Eq. (11) accounts for the development of prying forces in T-stubs as shown in failure modes 1 and 2, which should be replaced by 2.0 for mode 3 mechanism due to the absence of prying effect.

It has to be noted that the effect of bolt preloading is neglected in EN 1993-1-8, though bolt preloading has been shown to lead to considerable increase of the initial stiffness compared to the snug tightened condition as discussed in the previous section. Hence, two separate methods proposed by Jaspart [5] and Faella et al. [46] to take into account the stiffening effect of bolt preloading are considered herein. According to the method by Jaspart, a higher coefficient equal to 9.5 was adopted to replace the coefficient of 1.6 or 2.0 in Eq. (11) and a slightly lower factor of 0.85 instead of 0.9 was used for Eq. (10), while the Faella et al. method introduced the coefficient  $\psi$  in the calculation of the initial stiffness of the T-stub ( $K_t$ ), as defined in Eqs. (12) and (13).

$$K_{t} = \psi \frac{0.5E_{0,t}b_{\text{eff}}t_{f}^{3}}{m^{3}}$$
 (12)

$$\psi = 0.57 \left( \frac{t_{\rm f}}{d_{\rm b} \sqrt{m/d_{\rm b}}} \right)^{-1.28} \tag{13}$$

where the effective width of T-stub  $b_{\text{eff}}$  is equal to the bolt head diameter  $d_h$  plus twice the m value, and does not exceed the actual width b of T-stub.

The initial stiffness ( $K_0$ ) of the 40 tested stainless steel T-stub specimens was determined by regression analysis of the elastic range of the experimentally obtained F- $\Delta$  curves and is listed in Table 6 together with the corresponding numerically predicted values. Both experimental and numerical initial stiffness values were used to assess the aforementioned three calculation methods, with the predicted stiffness values also reported in Table 6. It has to be noted that the accuracy of the experimental values from the three test specimens with snug tightened bolts – S9, D8 and F10 is questionable due to the possible existence of gaps between plates, and hence the experimental stiffness values of these three specimens are excluded from the assessment of the methods. The average ratios of the test over the predicted initial stiffness values for the EN 1993-1-8 method and the Jaspart method are 1.52 and 1.40, with corresponding standard deviations equal to 0.92 and 0.99, respectively, indicating considerably underestimated initial stiffness for T-stubs with preloaded bolts, while the mean value of test over calculated ratio from the Faella et al.

method is equal to 1.20 with a much lower standard deviation of 0.49. Moreover, the calculated initial stiffness values from the Faella et al. method are also much closer to the numerically predicted results than those from the other two methods, and an average value of the FE over calculated ratio of 1.09 with a corresponding standard deviation of 0.16 is obtained. Thus, it is recommended that the Faella et al. method be used for calculating the initial stiffness of stainless steel bolted T-stub connections.

#### 4.2 Revised formulae for the plastic resistance

The comparison between experimental and codified plastic resistances discussed in section 3 has highlighted shortcomings in existing design methods, calling for the revision of the calculation formulae for the plastic resistance of stainless steel T-stubs. It has been found that the three typical failure modes of stainless steel T-stubs are consistent with the design formulae in EN 1993-1-8, yet the method specified in JGJ 82 does not distinguish between failure modes 1 and 2. Hence, the design formulae provided in EN 1993-1-8 were modified to obtain more accurate plastic resistance predictions for stainless steel bolted T-stubs. In view of the relatively small deformation values corresponding to the plastic resistance, it is expected that the static equilibrium equations that form the basis of design formulae in EN 1993-1-8 [3] and Demonceau et al. [20] can still be adopted, except that the material yield strength is replaced by the 3.0% proof strength  $\sigma_{3.0}$ , as indicated by the stress analysis presented in previous section. Hence, the proposed calculation formula for the plastic moment resistances of T-stub flange is given by

$$M_{\text{pl,i,Rd}} = \frac{t_{\text{f}}^2 f_{3.0}}{4} \sum l_{\text{eff},i} \quad i=1 \text{ or } 2$$
 (14)

By substituting the calculated plastic moments to the design equations including Eqs. (1), (2) and (6), the obtained plastic resistance predictions were compared against a total of 68 test and 147 FE data points, as plotted in Fig. 12 and listed in Table 7. It can be noted that only a few data points are below the line of 1.0, and the most unfavourable points correspond to the test results reported by Yang [28] and Lei [29], which can be explained by the fact that the nominal flange plate thickness values (usually higher than the actual values) were used to calculate the plastic resistances due to lack of measured thicknesses. The overall average value of the test/FE over the calculated resistance ratios is equal to 1.07 with a relatively small standard deviation of 0.07, indicating slightly conservative but satisfactory predictions for the plastic resistance of stainless steel T-stub connections.

#### 4.3 Reliability analysis

A reliability analysis of the revised calculation method was further carried out to verify the partial resistance factors by setting a target reliability index of 3.8 for ultimate limit state design with a reference service life of 50 years. Based on all available test and FE data points, the guidance provided in Annex D of EN 1990 [47] was followed herein by adopting the statistical data on material and geometric parameters of stainless steel elements reported by Afshan et al. [48]. The obtained key statistical parameters are listed in Table 8, where the correction factor b is taken as the slope of the least squares line for each failure mode,  $V_{\delta}$  is the coefficient of variation (COV) of the error term  $\delta_i$  for each data pair. It should be noted, however, that the over-strength value equal to 1.10 and a COV of 0.035 for the ultimate tensile strength were taken as the conservative values for both stainless steel grades, though the 3.0% proof strength of flange is used to predict the plastic resistance for both failure modes 1 and 2. A COV of 0.05 was adopted for geometric properties, and the  $V_r$  was calculated by combining the scatter effects due to the design model and the basic random variables. The required partial safety factor  $\gamma_{M0}$  value was found to be 1.17 for failure mode 1, higher than the current value of 1.1 recommended in EN 1993-1-4 [31], and this can be attributed to the use of conservative over-strength values for the ultimate tensile strength, and hence statistical data on the 3.0% proof strength are needed. The required partial safety factor value for mode 2 is equal to 1.07, which is less than both the current values of  $\gamma_{M0}$  and  $\gamma_{M2}$  involved in this failure mode, and the resulted  $\gamma_{M2}$  value for mode 3 is lower than the current value of 1.25, satisfying the related reliability requirements. The revised calculation method is therefore recommended for predicting the plastic resistance of stainless steel bolted T-stub connections.

#### 360 **Conclusions** 5

361

362

363

364

365

366

367 368

369

370

371

372

373

374

375

376 377

378

379

380

381 382

383

384

385

386

387

388

389

390

391

396

397 398

399

400

Augmenting previous experimental work, 13 monotonic loading tests on bolted stainless steel T-stubs in tension were conducted. All available test data on the plastic resistance of stainless steel T-stubs were collated and were used herein to evaluate the applicability of existing design methods for carbon steel T-stubs (i.e. EN 1993-1-8 and Chinese code JGJ 82) to stainless steel T-stubs; it was determined that they provide overly conservative predictions.

Numerical models were developed and validated against available experimental tests on stainless steel T-stubs in tension. The numerically predicted load versus deformation curves and failure modes were found to be in close agreement with the test curves, thus verifying the accuracy of the FE models. Further a comprehensive parametric study involving a total of 168 FE models was carried out to examine the effect of key parameters such as material grade, bolt preloading, bolt diameter and flange thickness on the T-stub strength and stiffness. It has been found that stainless steel T-stubs display identical failure mechanisms to the three typical modes given in EN 1993-1-8, except that the stresses at plastic flange yielding reaches up to the 3.0% proof strength due to the effect of strain hardening. Increasing the bolt diameter can considerably raise the tension resistance of T-stubs, especially for those displaying failure modes 2 and 3, and the introduction of bolt preloading results in a significant increase in the initial stiffness of T-stubs.

Based on the obtained test and numerical results, the calculation method by Faella et al. accounting for the bolt preloading effect was shown to provide much closer predictions for the initial stiffness of stainless steel bolted T-stub connections than the EN 1993-1-8 method and the Jaspart method. Meanwhile, revised calculation formulae for the determination of the plastic resistance of the T-stubs were proposed by replacing the material yield strength with the 3.0% proof strength within the framework of the design methods in EN 1993-1-8 as well as proposed extensions thereof by Demonceau et al. Since the use of the 3.0% proof strength  $\sigma_{3.0}$  allows for a rational exploitation of strain hardening consistent with experimental and numerical observations, the proposed method is shown to generate satisfactory predictions for the plastic resistance. The safety assessment of the revised calculation method has been further verified by a reliability analysis, and it is therefore recommended that the proposed design method be adopted for the design of stainless steel T-stubs.

#### Acknowledgements

The authors are grateful for the financial supports from the Natural Science Foundation of Hubei Province (Grant no. 2018CFB441), National Natural Science Foundation of China (Grant no. 51508424), the Fundamental Research Funds for the Central Universities (Grant no. 2042017gf0047) and the China Postdoctoral Science Foundation (Grant no. 2015T80832). The corresponding author is also grateful for the support from the Youth Talent Training Programme by Wuhan University in the year of 2018.

#### References

- 392 R. T. Douty, W. McGuire, High strength bolted moment connections, J. Struct. Div. ASCE 91(ST2) (1965) 101-128.
- 393 394 J. H. A. Struik, J. de Back, Tests on bolted T-stubs with respect to a bolted beam-to-column connection, Stevin Laboratory Report 6-69, Delft University of Technology, Delft, The Netherlands, 1969. 395
  - EN 1993-1-8, Eurocode 3: Design of steel structures Part 1.8: Design of joints, CEN, 2005.
  - [4] P. Zoetemeijer, A design method for the tension side of statically loaded, bolted beam-to-column connections, Heron 20 (1) (1974)
  - J. P. Jaspart, Recent advances in the field of steel joints column bases and further configurations for beam-to-column joints and beam splices, Chercheur qualifié du FNRS, Universite de Liege, Faculte des Sciences Appliques, 1997.
    - J. A. Swanson, R. T. Leon, Bolted steel connections: tests on T-stub components, J. Struct. Eng. ASCE 126(1) (2000) 50-56.
- 401 J. A. Swanson, D. S. Kokan, R. T. Leon, Advanced finite element modeling of bolted T-stub connection components, J. Constr. Steel 402 Res. 58 (2002) 1015-1031.
- 403 V. Piluso, C. Faella, G. Rizzano, Ultimate behavior of bolted T-Stubs – I: Theoretical model, J. Struct. Eng. ASCE 127(6) (2001) 404 686-693.

- 405 [9] V. Piluso, C. Faella, G. Rizzano, Ultimate behavior of bolted T-stubs II: Model validation, J. Struct. Eng. ASCE 127(6) (2001) 694–704.
- 407 [10] V. Piluso, G. Rizzano, Experimental analysis and modelling of bolted T-stubs under cyclic loads, J. Struct. Eng. ASCE 64(6) (2008) 655–669.

- 409 [11] A. M. Girão Coelho, F. S. Bijlaard, N. Gresnigt, L. Simões da Silva, Experimental assessment of the behaviour of bolted T-stub connections made up of welded plates, J. Constr. Steel Res. 60(2) (2004) 269–311.
  - [12] A. M. Girão Coelho, L. Simões da Silva, F. S. Bijlaard, Finite-element modeling of the nonlinear behavior of bolted T-stub connections, J. Struct. Eng. ASCE 132(6) (2006) 918–928.
  - [13] Z. Y. Wang, W. Tizani, Q. Y. Wang, Strength and initial stiffness of a blind-bolt connection based on the T-stub model, Eng. Struct. 32(9) (2010) 2505–2517.
    - [14] X. L. Liu, Y. Wang, M. H. Li, M. L. Han, Experimental study on the T-stub connections in steel structure, Journal of Xi'an Architecture and Technology University (Nature and Science Edition), 47(6) (2015) 848–853 (in Chinese).
    - [15] X. L. Liu, Y. Wang, M. H. Li, M. L. Han, Force analysis and numerical simulation of high strength bolts in T-stub connections of steel structure, Journal of Architecture and Civil Engineering, 33(2) (2016) 63–70 (in Chinese).
    - [16] M. S. Zhao, C. K. Lee, S. P. Chiew, Tensile behavior of high performance structural steel T-stub joints, J. Constr. Steel Res. 122 (2016) 316–325.
    - [17] C. Chen, X. Z. Zhang, M.S. Zhao, C. K. Lee, T. F. Chung, S. P. Chiew, Effects of welding on the tensile performance of high strength steel T-stub joints, Struct. 9 (2016) 70–78.
    - [18] H. C. Guo, G. Liang, Y. L. Li, Y. H. Liu, Q690 high strength steel T-stub tensile behavior: Experimental research and theoretical analysis, J. Constr. Steel Res. 139 (2017) 473–783.
    - [19] G. Liang, H. C. Guo, Y. H. Liu, Y. L. Li, Q690 high strength steel T-stub tensile behavior: Experimental and numerical analysis, Thin-Walled Struct. 122 (2018) 554–571.
    - [20] J. F. Demonceau, K. Weynand, J. P. Jaspart, C. Müller, Application of Eurocode 3 to steel connections with four bolts per horizontal row, In: Proceedings of the SDSS'Rio 2010 conference. Rio de Janeiro (2010) 199–206.
  - [21] M. Latour, G. Rizzano, A. Santiago, L. S. da Simões, Experimental analysis and mechanical modeling of T-stubs with four bolts per row, J. Constr. Steel Res. 101 (2014) 158–174.
  - [22] G. De Matteis, A. Mandara, F. M. Mazzolani, T-stub aluminum joints: influence of behavioural parameters, Comput. Struct. 78(1) (2000) 311–327.
  - [23] G. De Matteis, M. Brescia, A. Formisano, F.M. Mazzolani, Behaviour of welded aluminum T-stub joints under monotonic loading, Comput. Struct. 87(15) (2009) 990–1002.
  - [24] G. De Matteis, M. T. Naqash, G. Brando, Effective length of aluminum T-stub connections by parametric analysis, Eng. Struct. 41 (2012) 548–561.
  - [25] H. Xu, X. N. Guo, Y. G. Luo, Load-bearing capacity of aluminum alloy T-sub joints, Journal of Tongji University (Nature Science), 40(10) (2012) 1445–1451 (in Chinese).
  - [26] EN 1999-1-1: Eurocode 9: Design of aluminium structures Part 1.1: General structural rules, CEN, 2007.
  - [27] A. Bouchaïr, J. Averseng, A. Abidelah, Analysis of the behaviour of stainless steel bolted connections, J. Constr. Steel Res. 64(11) (2008) 1264–1274.
  - [28] C. Yang, Establishment of constitutive model at high temperatures for stainless steel bolts and study on mechanical behavior of its T-stub [Master's thesis], Chongqing University, China, 2017 (in Chinese).
  - [29] X. Lei, Experimental and numerical analysis on tensile behavior of welded stainless steel T-stub connections [Master's thesis], Chongqing University, China, 2018 (in Chinese).
  - [30] H. X. Yuan, S. Hu, X. X. Du, L. Yang, X. Y. Cheng, M. Theofanous, Experimental behaviour of stainless steel bolted T-stub connections under monotonic loading, J. Constr. Steel Res.152 (2019) 213–224.
  - [31] H.X. Yuan, S. Hu, X.X. Du, L. Yang, X.Y. Cheng, M. Theofanous, Corrigendum to "Experimental behaviour of stainless steel bolted T-stub connections under monotonic loading", J. Constr. Steel Res. 172 (2020) 105860.
  - [32] EN 1993-1-4, 2006+A1: 2015, Eurocode 3: Design of steel structures Part 1.4: General rules –Supplementary rules for stainless steels, CEN, 2015.
  - [33] M. Elflah, M. Theofanous, S. Dirar, H. X. Yuan, Behaviour of stainless steel beam-to-column joints Part 1: Experimental investigation, J. Constr. Steel Res. 152 (2019) 183–193.
  - [34] M. Elflah, M. Theofanous, S. Dirar, Behaviour of stainless steel beam-to-column joints—Part 2: Numerical modelling and parametric study, J. Constr. Steel Res. 152 (2019) 194–212.
  - [35] Y. Bu, Y. Wang, Y. Zhao, Study of stainless steel bolted extended end-plate joints under seismic loading, Thin-Walled Struct. 144 (2019) 106255.
  - [36] J.D. Gao, H.X. Yuan, X.X. Du, X.B. Hu, M. Theofanous, Structural behaviour of stainless steel double extended end-plate beam-to-column joints under monotonic loading, Thin-Walled Struct. 151 (2020) 106743.
  - [37] M. Theofanous, M. Elflah, S. Dirar, H. X. Yuan, Structural behaviour of stainless steel beam-to-tubular column joints, Eng. Struct. 184 (2019) 158–175.
  - [38] J. Wang, B. Uy, D. Li, Behaviour of large fabricated stainless steel beam-to-tubular column joints with extended endplates. Steel and Compos. Struct. 32(1) (2019) 141–156.
  - [39] JGJ 82, Technical Specification for High Strength Bolt Connections of Steel Structures, China Architecture and Building Press, Beijing, 2011 (in Chinese).
  - [40] American Institute of Steel Construction (AISC), Steel Construction Manual, Part 9, 14th ed, 2011.
  - [41] H. Hibbitt, B. Karlsson, P. Sorensen, ABAQUS Analysis User's Manual Version 6.10, Dassault Systèmes Simulia Corp.: Providence, RI, USA, 2011.
  - [42] M. Wang, Y. J. Shi, Y. Q. Wang, G. Shi, Numerical study on seismic behaviors of steel frame end-plate connections, J. Constr. Steel Res. 90 (2013) 140–152.
- 471 [43] N. Stranghöner, N. Afzali, P. de Vries, E. Schedin, J. Pilhagen, Slip factors for slip-resistant connections made of stainless steel. J.

472 Constr. Steel Res. 152 (2019) 235-245.

480

- 473 [44] J. P. Jaspart, R. Maquoi, Effect of bolt preloading on joint behaviour, In: Proceedings of the First European Conference on Steel 474 Structures (1995) 219-226.
- 475 [45] C. Faella, V. Piluso, G. Rizzano, Experimental analysis of bolted connections: snug versus preloaded bolts, J. Struct. Eng. ASCE 476 124(7) (1998) 765-774.
  - [46] C. Faella, V. Piluso, G. Rizzano, Structural steel semirigid connections: theory, design and software, CRC press, 2000.
- 477 478 479 [47] EN 1990:2002+A1:2005, Eurocode-Basis of structural design, CEN, 2010.
  - [48] S. Afshan, P. Francis, N.R. Baddoo, L. Gardner, Reliability analysis of structural stainless steel design provisions, J. Constr. Steel Res. 114 (2015) 293-304.

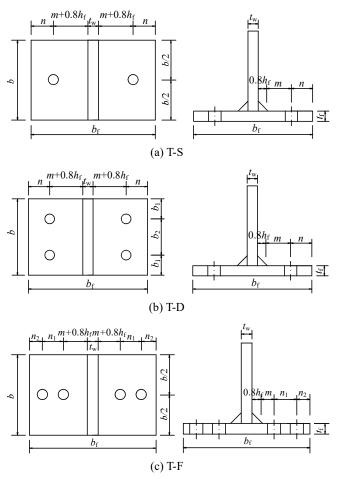


Fig. 1. Geometric details of T-stub specimens

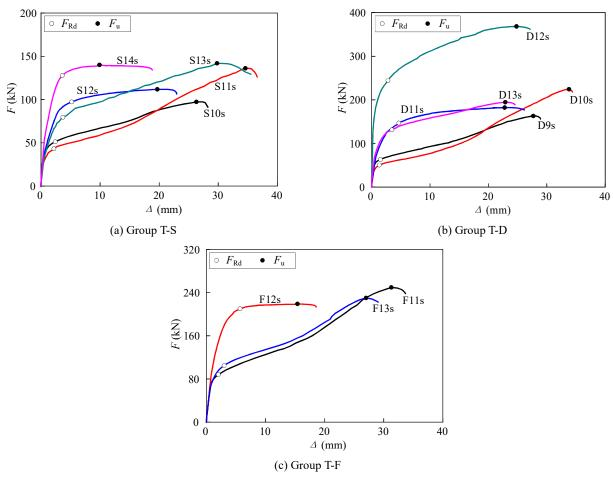


Fig. 2. Experimental F- $\Delta$  curves of the tested T-stub specimens

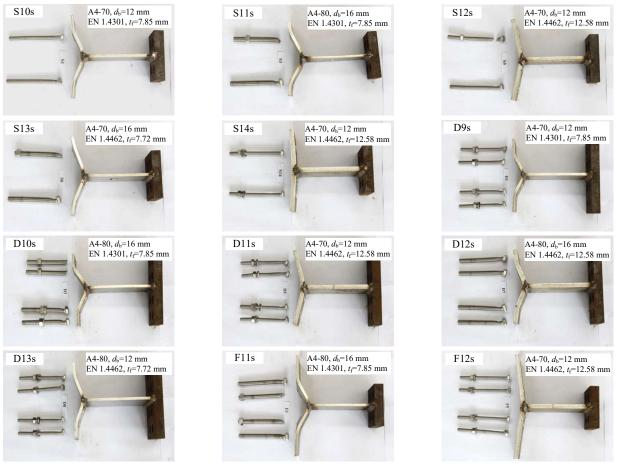


Fig. 3. Deformed shapes of the test specimens

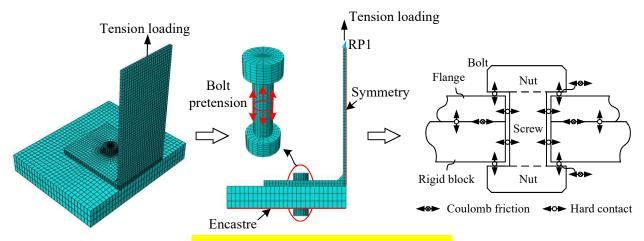


Fig. 4. Boundary and contact conditions of FE models

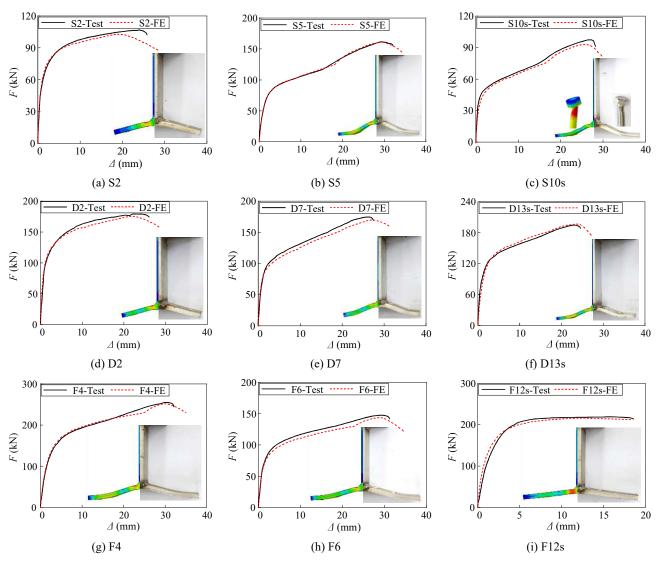


Fig. 5. Comparison of F- $\Delta$  curves and deformed shapes from FE modelling and tests

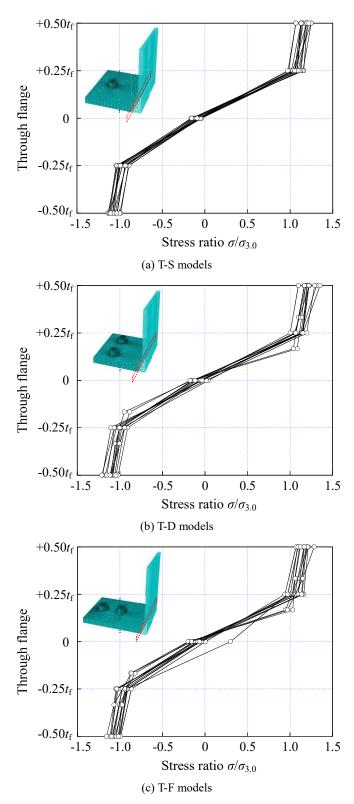
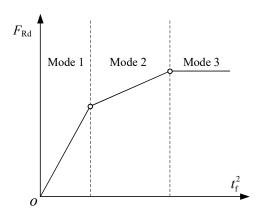


Fig. 6. Numerical stress distributions through flange thickness located close to flange-to-web intersection



**Fig. 7.** Relationship between  $F_{\rm Rd}$  and  $t_{\rm f}^2$  according to EN 1993-1-8

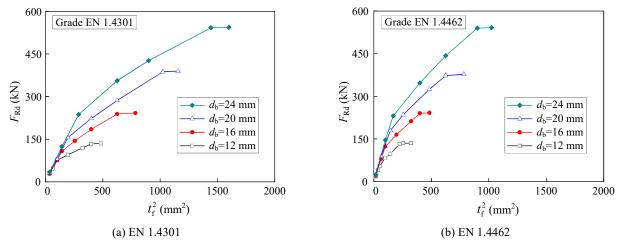


Fig. 8. Influence of bolt diameter  $d_b$  and material grade

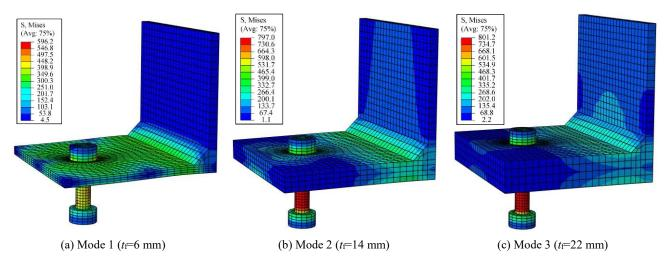


Fig. 9. The three typical failure modes of stainless steel T-stubs

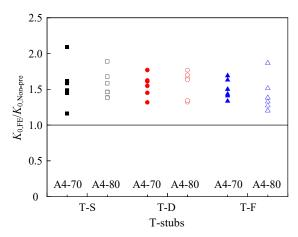


Fig. 10. Comparison between numerical simulations with and without bolt preloading

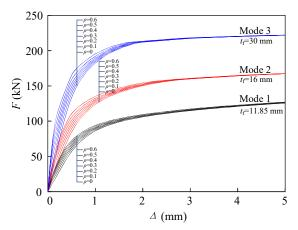


Fig. 11. Influence of bolt preloading ratio  $\rho$ 

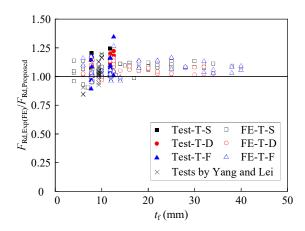


Fig. 12. Comparison of predictions from the revised formulae with available test and numerical results